



Copyright © 2016 Singh and Pandey

This is an Open Access article distributed under the terms of the Creative Commons Attribution License (<http://creativecommons.org/licenses/by/2.0>), which permits unrestricted use, distribution, and reproduction in any medium, provided the original work is properly cited.

## ORIGINAL RESEARCH

# Structural Modeling of Human *Tyrosinase* Protein Using Computational Methods

Pankaj SINGH<sup>1\*</sup>, Khushhali M PANDEY<sup>1</sup>

<sup>1</sup>Department of Biological Science and Engineering, Maulana Azad NIT-Bhopal

\*Corresponding Author email: [singhpankaj2116@gmail.com](mailto:singhpankaj2116@gmail.com)

• Received: 29 August 2015 • Revised: 10 October 2015 • Accepted: 18 October 2015 • Published: 16 January 2016 •

## ABSTRACT

*Tyrosinases* have a ubiquitous presence among all domains of life. They are an essential and most vital component for pigmentation, wound healing and primary immune response. Their active site contains antiferromagnetically coupled copper ions, CuA and CuB, which is coordinated by six histidine residues. This arrangement is known as “type 3 copper centers” and is found across *Tyrosinases*, catecholoxidases and haemocyanins. The copper pair of *Tyrosinases* binds one molecule of atmospheric oxygen to catalyze two different kinds of enzymatic reactions namely the cresolase activity which is ortho-hydroxylation of monophenols and the catecholase activity oxidation of o-diphenols to o-diquinones. The formation of melanins takes place from L-tyrosine via L-dihydroxyphenylalanine (L-dopa). Since the tertiary structure of *Tyrosinase* has still not been elucidated, researchers have a hard time in understanding the complicated hydroxylation mechanism at the active center. Recently researchers have experimentally determined the bacterial *Tyrosinase* structures in *Streptomyces* and *Bacillus*, although no such attempt has been taken towards solving the structure of the human *Tyrosinase* protein despite of the prevailing knowledge regarding the protein. In our current work, we have tried to model the tertiary structure of the human *Tyrosinase* protein using template based (Homology) and non-template based (*ab initio*) modeling methods. We have also compared the scores of our model with that of the existing bacterial model and also tried to study its behavior using Molecular Dynamics techniques at a small scale.

**KEY WORDS:** *Tyrosinase*, type 3 copper centers, tertiary structure

## Introduction

Melanin synthesis is carried out by *Tyrosinase* protein family, which comprises, *Tyrosinase* related protein 1 (TRP1 or Tyrp 1) and *Tyrosinase* related protein 2 (TRP2 or DCT or Tyrp 2). *Tyrosinases* are the best studied multi-copper oxygenase. It uses its binuclear copper center to catalyze the hydroxylation of tyrosine to dihydroxyphenylalanine (DOPA) i.e., tyrosine hydroxylase activity (Lerner *et al.*, 1949). This step is considered as the rate limiting step in the synthesis of melanin. *Tyrosinase* also catalyzes the subsequent oxidation of DOPA to DOPAquinone (DOPA oxidase activity) and further downstream products 5, 6-dihydroxyindole (DHI) and 5,6-dihydroxyindole-2-carboxylic acid (DHICA) into eumelanin precursors and indole-5,6-

quinone carboxylic acid, respectively (Korner and Pawelek, 1982; Lerner *et al.*, 1949) (Fig 2).

*Tyrosinase* or Ty contains two copper ions that are closely spaced within the protein matrix. CuA and CuB are the two copper binding regions, which have been found in all *Tyrosinases*. Each of these regions contains three conserved histidine residues, which coordinate to a pair of *Tyrosinase* with both molecular oxygen as its substrates. A close homology has been found between the CuA and CuB region of Ty and the corresponding CuA and CuB regions of Hemocyanins (Hcs), which are oxygen carriers found in many molluscs and arthropods and the catechol oxidases (COs) that oxidize diphenols but do not show the Ty

hydroxylation activity. These proteins also contain a dinuclear copper site and share strong functional, mechanistic and structural similarities with the *Tyrosinases*. Together the Tys, Hcs and COs are classified as “type-3” copper proteins.

The present study deals with predicting the structure of the type-3 copper protein *Tyrosinase* (Ty). The 3D structure has been emphasized due to the well-known fact that a protein is functional in its native form which is the tertiary structure itself. Anfinsen’s theory of protein folding established the foundation for solving the protein structure prediction problem. The methods for computational structure prediction have been discussed briefly and will be elaborated in the upcoming chapters. The function of the enzyme has been described in the previous sections, to summarize the enzyme catalyses the hydroxylation of monophenols to give o-diphenols and the oxidation of o-diphenols to the corresponding quinones. These quinones are the reactive precursors in the synthesis of melanin pigments that fulfill various roles in different organisms. Ty occurs widespread in nature and can be found through the phylogenetic tree. The crystal structure for Ty is already available for bacteria such as *Bacillus megaterium* and *Streptomyces* in the PDB database but no such structure information exists for Human or other animal *Tyrosinases*. The present work deals with elucidating a tertiary structure for human *Tyrosinase* using computation based structure modeling method.

Mutations that abolish Ty activity block the melanogenic pathway which leads to oculocutaneous albinism type 1 (OCA1, OMIM 203100), an autosomal recessive disorder characterized by absence of pigment in hair, skin and eyes (Oetting, 2000). In addition to mutation to hot spots (copper-binding domains) virtually the entire coding sequence of the gene is susceptible to mutations. Presently over 200 mutations in Ty gene have been associated with albinism, these mutation include missense, nonsense, frameshift and splicing abnormalities. Apart from these the melanocyte pathway has generated a lot of interest and enthusiasm in researchers.

Human Ty 3D structure has been a fascinating as well a challenging area as, although much is known about Ty yet the very few attempts have been made towards its structural aspect. The active site has been elucidated but the whole 3D structure has still not been modeled either structurally or

experimentally. In this study an attempt has been made to model the Ty structure using computational methods preferably Homology and Ab initio methods. Apart from the modeling, we have also tried to study the behavior of the protein using molecular dynamics methods.

## Materials and Methods

### Hardware

1. Pentium dual core processor.
2. 3 GB RAM (or more)
3. High speed Internet facility.
4. Super Computing facility for Molecular Dynamics (not procured).

### Software

1. Windows Vista/XP/7/Linux operating system.
2. Modeler 9V8 (9V9), SWISS-MODELLER, VEGAzz.
3. ZMM-MVM, Moil, VMD, NAMD, NOC.
4. RASMOL, JMOL, Pymol.
5. AMBER/CharmM (not procured).

### Miscellaneous

1. Books and journals.
2. Open web sources etc.

### Retrieving the target sequence

As from literatures, the Human *Tyrosinase* was reported to contain 529 amino acid (aa). Hence the first task was to search for the required protein in the available databases. The target protein sequence, which we wanted to model, was retrieved from the NCBI database. The search for the sequence was limited to protein database for Human and *Tyrosinase*.

Then according to information available from the previous works, we were able to select the GenBank protein sequence with Accession Number: AAB60319.1, from the several available sequences from both Eukaryotes and Prokaryotes. The sequence was then downloaded in the FASTA format and saved in a specific destination for the structure prediction work.

### Searching for template sequences

Once done with finding the target sequence, our next aim

was to find the corresponding template sequences whose structure was already available in the PDB database. This was indeed the main step for the template based structure prediction. We mainly relied in the BASIC LOCAL SEARCH ALIGNMENT TOOL (BLASTp) available with NCBI.

The First BLASTp search was carried out using default parameters thereafter the other BLASTp searches were carried out which excluded the Eukaryotes and also involved position specific iterative BLAST (PSI-BLAST). We also searched for the template sequences in PDB and other databases.

### Homology modeling

Once the target and the template structures were obtained our next aim was to construct a homology model of the target sequence using the template sequences.

For this various tools and software's both offline and online are available freely or commercially. We specifically chose the open source homology modeling tools. Following tools are available:

1. Modeller 9v9 & 9v8 (standalone tool).
2. Easy Modeller (a GUI to Modeller).
3. SWISS-MODEL (Online server).
4. FOLD X (standalone tool).
5. Robetta (online web server).
6. 3D JIGSAW (online web server), etc.

Although we submitted our query on the all the above web servers yet we solely relied on the model modeled using Modeller 9v9 & 9v8. We followed the basic protocol for the modeling purpose using Modeller 9v9. Although two approaches were followed using different parameters which were as follows:

Using single template without including the HETATOMS.

Using Single template using HETATOMS.

Using multiple templates without HETATOMS.

Using multiple templates including HETATOMS. Initial model thus obtained was then visualized using an open source protein visualizing software. Following protein structure visualizing tools are available free of cost for the researchers:

Rasmol

Jmol

Pymol

Vegazz (both visualizing and modeling) etc.

VMD We made use of Vegazz, VMD and Rasmol for visualizing and editing the initial model. The next step in the homology modeling process was to evaluate the model. Various online web servers and tools are available for evaluating a model. Following are the online tools available for evaluating the model:

We relied on Prosall, ERRAT and VERIFY3D results for model evaluation.

### Ab initio Methods

To validate the accuracy of the homology model, we used another structure prediction technique which did not required any template structure rather was based upon the first principles of physics.

We constructed the protein chain using the amino acid sequence information using Marvin Sketch/Chem Sketch (in this case we preferred Marvin Sketch) tools which was freely available in the standalone version. Now, we had to construct the 3D structure of this model using these tools itself. We optimized this initial model and converted it into the 3D form using the option available in these software's.

The next step was to predict the positions in the protein structures where the Copper molecules bind. Although most information was gathered from the literatures yet the information regarding the exact position of copper binding was not available in the literatures as well. So we relied on the Support Vector Machine (SVM) based web servers to predict the metal binding sites on the protein chain. Various free tools are available on webs that have been used to predict the metal binding site in a protein structure. Following are the tools to name a few:

1. MetSite
2. Ched
3. MDB (metalloproein database).
4. Probis
5. Disulfide
6. Metaldetector
7. GRID
8. Par-3D
9. Zinc Binding site predictor.

We used MetSite, Ched, MetalDetector, MDB to predict the metal binding sites. After predicting the binding sites, our next task was to insert the copper at the respective position for which we needed commercially available tools Gaussian and Amber.

After insertion of copper at the respective position by specifying the coordinate by Gaussian followed by application of AMBER force field to optimize the binding and to apply the force field. The model was again verified for accuracy using Prosall, Procheck and Verify 3D.

#### **Molecular dynamics study of the model**

After modeling the protein structure and evaluating our model, we moved further to study the dynamics of the protein molecule. As already explained in chapter 1 & 2, the dynamic behavior of a protein is as important as is the structure for the study of its function.

Various tools and software's are available both commercially and open source for the molecular dynamics study of the protein structure. We used the open source software's which were among the following:

1. Tinker
2. VMD-NAMD
3. Vegazz
4. Moil
5. Chimera
6. Ball view
7. NOC etc.

Although we worked on all of these tools but relied more on moil, VegaZZ and VMD-NAMD. The parameters were set according to those available in literature and as described in the previous sections.

## **Results**

#### **Human Ty protein translocation, maturation and transport events**

Prior to model the Human Ty using computational methods, it was indeed necessary for us to enhance our understanding about the translation of Human Ty gene and the processes behind its translocation from nucleus, its maturation and transport. This step was achieved by going through the available literatures from different researchers. Although we were aware that the Human Ty is 529 amino acid sequence, but was this the exact length which folded into the functional protein or else did it contain certain length that guided it to the destination where it could mature and fold properly for the desired function? We therefore describe the first steps that we implemented to develop a computational model for the Human Ty which often designate as the 529 amino acid

sequence!

Human Ty is a type I membrane glycoprotein that contains 529 amino including an 18 amino acid N-terminal signal peptide sequence (as in figure). The human and mouse Ty have been found to be highly conserved with almost 85% sequence identity (Kwon *et al.*, 1988 a, b). The mature protein can be divided into three domains: (1) The N-terminal 455 amino acid luminal ectodomain; (2) a single transmembrane domain; and (3) a C-terminal cytoplasmic tail.

The enzymatic activity is possessed by the ectodomain region. It has seven consensus N-linked glycosylation sites and 17 Cys residues. One Cys residue is located in its cleaved signal sequence that leaves behind the rest of the 15 Cys residues available for disulfide bonding under the oxidizing conditions of the endoplasmic reticulum (ER) lumen. Six of the seven glycosylation sites are conserved in mouse Ty while all the luminal Cys are conserved. The N-linked glycosylation sites are spaced throughout the luminal domain, while the Cys residues are concentrated in three Cys-rich clusters.

Both human and mouse Ty have a single 26 amino acid hydrophobic transmembrane domain which is approximately 70% conserved. The transmembrane domain anchors Ty in the melanosome membrane with the N-terminal ectodomain facing the lumen. Mouse Ty is four amino acid longer than human Ty, because of an extension of the C-terminal cytoplasmic tail. The C-terminal tails of both human and mouse Ty possess two well studied intracellular targeting signals. These signals include a di-leucine (LL) motif and a tyrosine based motif (YXXB, where B is a hydrophobic residue) (Blagoveshchenskaya *et al.*, 1999; Calvo *et al.*, 1999; Honing *et al.*, 1998; Simmen *et al.*, 1999). The previous numbering of the Ty residue started with Met residue at position number 1 and the signal sequence consisted of 18 residues from 1 to 18. Thus the residue from where the protein gets cleaved is the 18 the residue from Methionine i.e., the Glycine residue, that makes His the first amino acid in the Ty protein.

Translocation of Ty into the ER lumen is guided by its N-terminal cleavable signal sequence. The signal sequence binds to the signal recognition particle (SRP), which targets the ribosome nascent chain complex to the ER membrane by binding to its cognate SRP receptor. This binding

Accession	Description	Max score	Total score	Query coverage	E value	Links
<a href="#">ABM82392.1</a>	dopachrome tautomerase (dopachrome delta-isomerase, tyrosine-related prote	<a href="#">390</a>	390	97%	1e-106	<a href="#">G</a>
<a href="#">ACC85108.1</a>	tyrosinase [Bacillus megaterium]	<a href="#">128</a>	128	62%	1e-27	
<a href="#">3NM8_A</a>	Chain A, Crystal Structure Of Tyrosinase From Bacillus Megaterium >pdb 3NM8	<a href="#">128</a>	128	62%	1e-27	<a href="#">S</a>
<a href="#">YP_003598579.1</a>	tyrosinase [Bacillus megaterium DSM 319] >gb ADF40229.1  tyrosinase [Bacillu	<a href="#">128</a>	128	63%	2e-27	<a href="#">G</a>
<a href="#">3NQ5_A</a>	Chain A, Crystal Structure Of Tyrosinase From Bacillus Megaterium R209h Muta	<a href="#">128</a>	128	62%	2e-27	<a href="#">S</a>
<a href="#">YP_003563841.1</a>	tyrosinase [Bacillus megaterium QM B1551] >gb ADE70407.1  tyrosinase [Bacill	<a href="#">127</a>	127	62%	3e-27	<a href="#">G</a>
<a href="#">NP_841294.1</a>	tyrosinase [Nitrosomonas europaea ATCC 19718] >emb CAD85152.1  Tyrosina	<a href="#">123</a>	123	57%	5e-26	<a href="#">G</a>
<a href="#">ZP_06476284.1</a>	tyrosinase [Frankia symbiont of Datisca glomerata] >gb AEH10743.1  Monophe	<a href="#">119</a>	119	56%	1e-24	
<a href="#">ZP_07275833.1</a>	tyrosinase [Streptomyces sp. SPB78] >gb EFL04202.1  tyrosinase [Streptomy	<a href="#">117</a>	117	58%	2e-24	
<a href="#">ZP_07978258.1</a>	tyrosinase [Streptomyces sp. SA3_actG]	<a href="#">117</a>	117	58%	2e-24	
<a href="#">ZP_08450673.1</a>	putative tyrosinase [Streptomyces sp. Tu6071] >gb EGJ72902.1  putative tyro	<a href="#">116</a>	116	58%	6e-24	
<a href="#">YP_001865661.1</a>	tyrosinase [Nostoc punctiforme PCC 73102] >gb ACC80718.1  tyrosinase [Nos	<a href="#">113</a>	113	58%	5e-23	<a href="#">G</a>
<a href="#">ZP_06822062.1</a>	tyrosinase [Streptomyces sp. SPB74] >gb EDY46797.1  tyrosinase [Streptomy	<a href="#">112</a>	112	58%	1e-22	
<a href="#">ZP_07312931.1</a>	tyrosinase [Streptomyces griseoflavus Tu4000] >gb EFL41300.1  tyrosinase [S	<a href="#">111</a>	111	46%	1e-22	
<a href="#">YP_001825758.1</a>	ortho-aminophenol oxidase [Streptomyces griseus subsp. griseus NBRC 13350]	<a href="#">108</a>	108	46%	1e-21	<a href="#">G</a>
<a href="#">YP_001505111.1</a>	tyrosinase [Frankia sp. EAN1pec] >gb ABW10205.1  tyrosinase [Frankia sp. EA	<a href="#">108</a>	108	62%	2e-21	<a href="#">G</a>
<a href="#">ZP_06410499.1</a>	Monophenol monooxygenase [Frankia sp. EUN1f] >gb EFC86710.1  Monopheno	<a href="#">108</a>	108	49%	2e-21	
<a href="#">YP_710815.1</a>	putative tyrosinase [Frankia alni ACN14a] >emb CAJ59206.1  putative Tyrosina	<a href="#">107</a>	107	49%	2e-21	<a href="#">G</a>
<a href="#">NP_826539.1</a>	tyrosinase [Streptomyces avermitilis MA-4680] >dbj BAB69182.1  putative tyro	<a href="#">106</a>	106	43%	4e-21	<a href="#">G</a>
<a href="#">BAA37085.1</a>	MelC2 [Streptomyces griseus]	<a href="#">106</a>	106	46%	6e-21	
<a href="#">ZP_06914821.1</a>	tyrosinase [Streptomyces sviveus ATCC 29083] >gb EDY60306.1  tyrosinase [	<a href="#">105</a>	105	59%	1e-20	
<a href="#">YP_479355.1</a>	tyrosinase [Frankia sp. Cc13] >gb ABD09626.1  tyrosinase [Frankia sp. Cc13]	<a href="#">105</a>	105	58%	1e-20	<a href="#">G</a>
<a href="#">ZP_06578937.1</a>	tyrosinase [Streptomyces ghanaensis ATCC 14672] >gb EFE69398.1  tyrosina	<a href="#">105</a>	105	43%	1e-20	
<a href="#">ZP_04688134.1</a>	tyrosinase (monophenol monooxygenase) [Streptomyces ghanaensis ATCC 146	<a href="#">105</a>	105	43%	1e-20	
<a href="#">NP_626934.1</a>	tyrosinase (monophenol monooxygenase) [Streptomyces coelicolor A3(2)] >ref	<a href="#">104</a>	104	44%	2e-20	<a href="#">G</a>
<a href="#">ZP_07303866.1</a>	tyrosinase [Streptomyces viridochromogenes DSM 40736] >gb EFL32235.1  ty	<a href="#">104</a>	104	44%	2e-20	

Figure 1: BLAST results on excluding the eukaryotes

positions the ribosomal protein exit site onto the Sec61 channel to provide a direct route from the biosynthetic machinery into the ER lumen. The hydrophobic nature of the signal sequence creates an N-terminal tether or an additional transmembrane domain for Ty prior to its cleavage by the signal sequence cleavage peptidase. The early maturation events on Ty were studied by simulating the co-translational processes using ribosomal –arrested chains of increasing lengths (Wang *et al.*, 2005).

Human Ty is heterogeneously glycosylated with either six or all seven of its glycosylation sites being occupied (Ujvari *et al.*, 2001). The hypoglycosylation at Asn-272 (Asn-Gly-Thr-Pro) is caused by the proximal Pro at position 275. Pro

residues also inhibit the transfer reactions if they lay near the consensus site, in contrast Mouse Ty lacks a hypoglycosylated site at Asn272. Reports do suggest that the glycosylation of Ty is cell dependent. Glycosylation is indeed an essential step for Ty activity, this was shown glycosylation was inhibited using tunicamycin which led to improper Ty maturation and loss of its enzymatic activity (Imokawa and Mishima, 1981; Mishima and Imokawa, 1983; Takahashi and Parsons, 1992b). Researchers have shown that two classes of molecular chaperones in ER interact with *Tyrosinases* and aid in its maturation. One of them is an ER Hsp70 family member BiP which performs variety of functions in the maturation and regulation of protein. It is also



the first chaperone that associates with Ty. BiP achieves this task by recognizing unfolded regions containing hydrophobic residues (Fewell *et al.*, 2001; Flynn *et al.*, 1991). The second family of ER chaperones includes Calnexin and Calreticulin. They directly bind to the hydrophilic modification. Together these chaperones assist in proper maturation of Ty. The disulfide bonding in Ty begins co-translationally with the cleavage of signal peptide. The disulfide bond formation is an oxidation reaction catalyzed by protein disulfide isomerase (PDI) members present in the ER (Erp57). Erp57 appears to serve as the catalyst for oc- and post-translational oxidation of Ty.

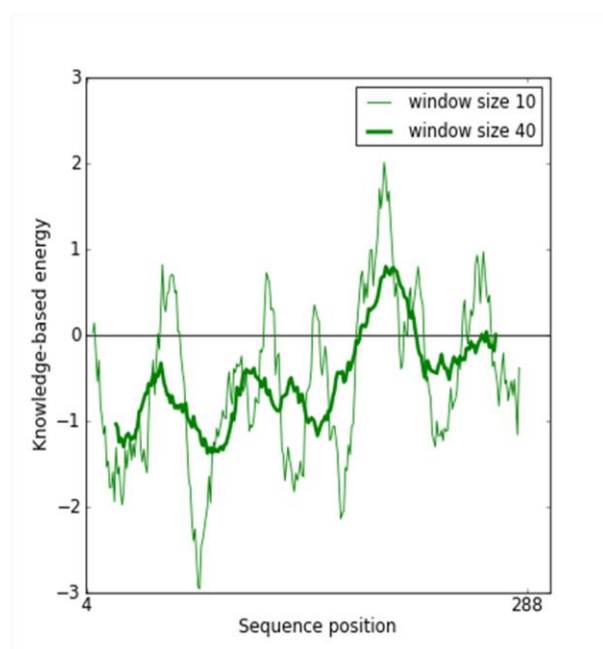


Figure 2: ProSA quality model for *B. megaterium*

The quaternary structure of Ty appears to involve both homo- and hetero- oligomeric interactions. This homodimer is formed after the proper folding in the ER, prior to its transport to the Golgi body (Francis *et al.*, 2003). It was concluded that the tyrosine dimerization required proper folding as the Ty misfolding mutant TYR (C71R) failed to form an oligomer (Francis *et al.*, 2003). This dimerization requires the participation Tyrp1 as the homodimerization failed in the Tyrp1 (C86Y) defective melan-b- cells. This was the experimentally proved by gel filtration chromatography and electrophoresis (Jimenez Cervantes *et al.*, 1998). Once matured in the ER, Ty is transported via Golgi bodies (shown in figure). (Ning Wang and Daniel N. Hebert).

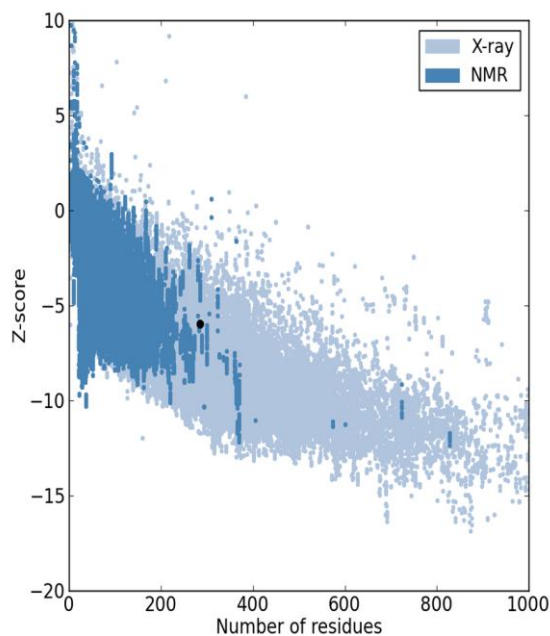


Figure 3: Z -score of *Bacterium megaterium*

#### Active site structure of mammalian Ty

In bacterium, active site of Ty contains an oxygen molecule bonded in side-on coordination between two copper ions (Matoba *et al.*, 2006). Each of the copper ions is coordinated by three His residue in the protein matrix. These His residues are located in two His- rich regions named CuA and CuB. Although both sites are highly similar in mouse Ty and Ty related proteins (mTyr and mTyrsps), catechol oxidase of sweet potato (ibCO) and bacterial Ty (sTyr), the conservation is higher in the CuB site. The engagement of these sites in copper binding has been experimentally demonstrated using site directed mutagenesis in Human and mouse Tys (Olivaries *et al.*, 2002).

Homology modeling of mouse Ty based on recently published crystal structures of non-mammalian Tys provides an active site model accounting for loss of function mutations. According to the model, the copper binding histidines are located in a helix bundle comprising four densely packed helices. A loop containing M374, S375 and V377 connects the CuA and CuB centers, with the peptide oxygen of M374 and V377 serve as hydrogen acceptors for the NH- groups of the imidazole rings of the copper binding His 367 and His 188. Hence, this loop was identified to be crucial for the stability of the active site architecture. The –OH group in S380 contributes to the correct orientation of

M374, and the substitution of V393 for a bulkier phenylalanine sterically impedes correct side chain packing at the active site. Thus these results indicate the necessity of adjacent amino acids apart from the Histidine residues at the active sites.

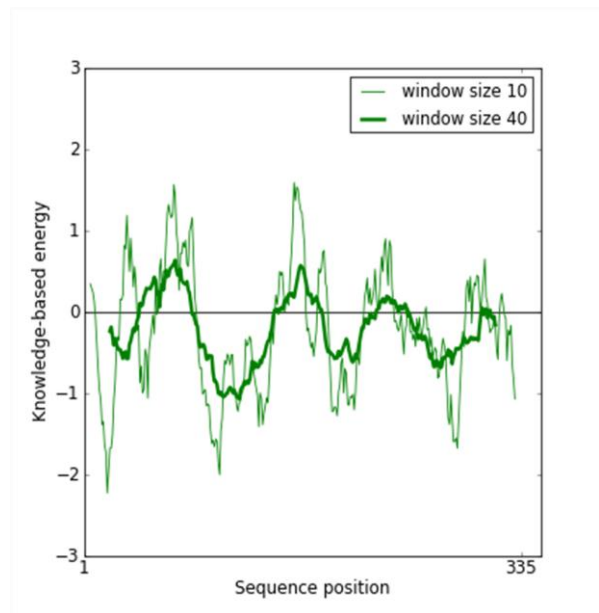


Figure 4: ProSA result for Human Tyrosinase

#### Homology modeling

The target, which was retrieved from the NCBI protein database, was aligned with template sequence using the Multiple sequence alignment tool Clustal W2/X2 (standalone version). This sequence was subjected to homology modeling using the modeler9V9 and other tools as mentioned. The difficulty in the homology modeling occurred as the target Human Ty sequence that we used was 529 aa, which contained an 18 aa signal sequence and the chain is also cleaved at 470-480 aa position.

So, two approaches still arouse, either we should consider the total 529 aa sequence for developing our model or else shall we consider the region after the first 18 residues and prior to the 470th aa position? We considered both the possibilities for developing the model using the modeler script and other web based/standalone tools, using the different parameters discussed previous sections. Different models were obtained, which were then verified using the web based tools for their efficacy and correctness. The local energy profile and the z-score value was analyzed using ProSA and the structural analysis results were based on the output from WHATIF. Although many models were verified,

here we discuss only one model.

This protein was modeled using the *B.megaterium* protein structure (PDB code 3NM8) as template. The copper molecules were inserted using two approaches: 1) directly by modeler using the HETATOM script. 2) The model was first developed using the modeler, the copper was then inserted by specifying the coordinates and restraints using Gaussian, which was further simulated using the AMBER force fields. The models have been shown in the figures along with their energy profiles.

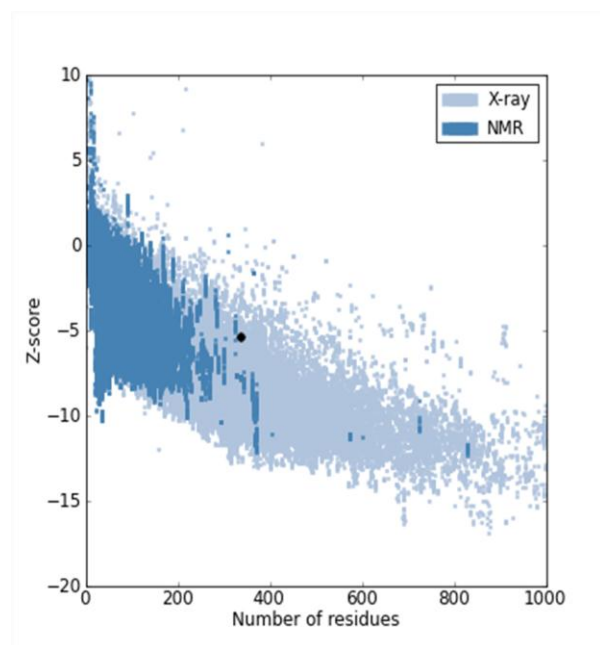


Figure 5: Z-Plot for Human Tyrosinase. Note that the bacterial and human model shows almost the same z-score

#### Ab initio modeling

The ab initio model was constructed using the Marvin Sketch tool which is freely available for academic users. This model was constructed using the sequence information of the human Ty protein. This model was a straight chain model in the 2D view.

The Ligand (copper) binding sites were predicted using the SVM (Machine learning tools) available online. As from the information from the literatures we basically expected the Histidine residues in the active site, which was confirmed from the results from these tools as well. We were now confused for constructing the active site from more than six histidine residues, as the literature suggested and confirmed the presence of only six histidine residues at the active site. We selected 6 residues out of the available 8-10 binding

sites. The selection of the histidine residues was based on the scores provided by the tools. The results for the binding site affinities of the residues have been shown in a tabular form as well as a screen shot from different web servers. Once the histidines residues involved in binding was predicted, we inserted copper using the bonding options available in Marvin Sketch software. The copper was inserted at the desired position but we could not optimize the energy and the coordinates of the metalloprotein molecule due to the unavailability of the supercomputing facility for molecular dynamics study. The 2D ab initio model has been shown in the figure.

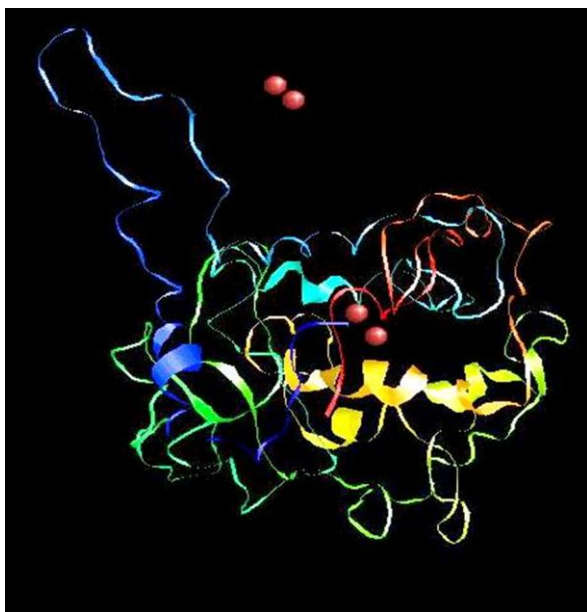


Figure 6: Computational model of Human Tyrosinase using modeler

### Discussion

The proposed model is based on homology study and ab initio methods using the information from the literatures. The mode shows a z- score value of 5.4 which is in accordance with the B. megatrium z- score value 5.98. The active site contains 6- His residues which are bound to two copper molecules surrounded by a loop that contains Met374, Ser 375 and Val 377, which connects CuA and CuB centers with the peptide oxygens of Met 374 and Val 377 for –NH group of imidazole rings of Cu- binding His 367 and His-180. In most of the case His is stabilized by a Cys-His bridge. Since mTy and sTy lack a Cys near the active site, the sTy should be used as a template rather than bTy.

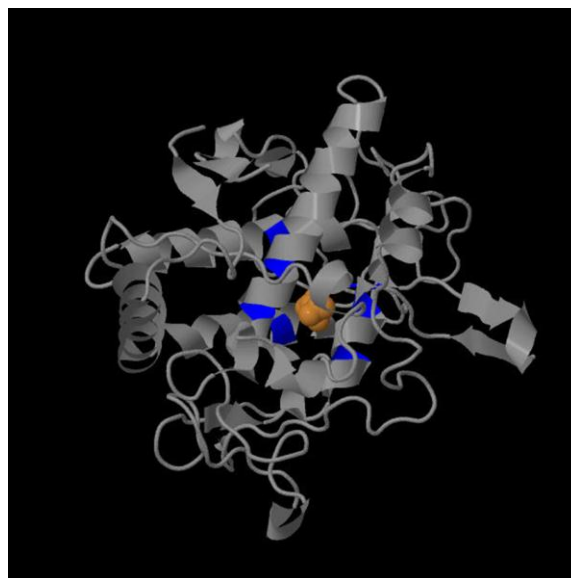


Figure 7: Another model predicted by 3D ligandsite server

There are almost 13 His residues present in the protein sequence, out of which the two Cu atoms bind with only 6 residues, in ab initio study this problem was highly complicated. So, the residues were selected by comparing the scores and preferences allotted by the Machine Learning tools. Also we relied totally on literature to match up with our ab initio results. Each of the copper-binding sites in a type 3 copper proteins is coordinated by three His residues. The CuA site of Ty is comprised of His162, 184, and 193, while the CuB site involves His345, 349, and 371 (Huber and Lerch, 1988; Muller *et al.*, 1988; Spritz *et al.*, 1997). These six His residues are conserved in Ty through a variety of species.

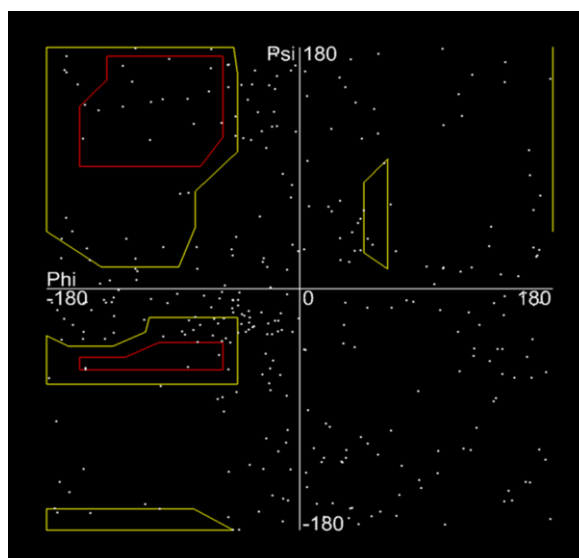


Figure 8: Ram Chandra Plot for Human Tyrosinase protein



The CuA site of bacterial and human Ty display 42% and 53% sequence identity and similarity and the CuB site have 42% and 73% sequence identity and similarity, respectively (van Gelder *et al.*, 1997). Secondary structure predictions and homology to copper proteins with known structures indicated that the CuA and CuB regions contain an  $\alpha$ -helical bundle creating a hydrophobic pocket near the protein surface (Garcia Borrón and Solano, 2002; van Gelder *et al.*, 1997). Some workers have even reported that the Ty active center is flexible during catalysis (Yasuyuki Matoba *et al.*, 2005), which we have not studied in our model. Also the exact coordinates of the CuA and CuB can differ from the actual arrangement due unavailability of practical evidence regarding the exact binding site. Another challenging aspect towards the computational structure prediction is the lack of information regarding the protein chain folding and insertion of the metal atom in the active site. This has been a topic of debate that whether protein folds first or the protein folding takes place after the metal ion has been included in the active site.



**Figure 9:** An *ab initio* model for Human tyrosinase using Marvin Sketch

We have tried to check both possibilities although an attempt to solve this problem faces the limitation of computational power and specific force field parameters. Another aspect that we had tried and is still under trial is the molecular dynamic studies of the Ty molecule. Although recently some workers have simulated the oxy form of the

protein using LFMD (ligand field molecular dynamics) for 16ns, where they have translated their type 3 copper force field for the peroxo-bridged  $[\text{Cu}_2\text{O}_2]^{2+}$  units which were translated from MMFF to AMBER format using a new charge scheme. The LMFD has been able to distinguish clearly between equatorial and axial Cu-N distance (Robert J Deeth and Christian Diedrich, 2010). Another important aspect of the active structure of the Ty protein is that this protein may exist as dimer (as in bacteria), tetramers/hexamers (as in arthropods). Again this oligomer formation may also be essential feature of Human Ty for activity, hence much more needs to be predicted regarding the active form of the Human *Tyrosinase* protein.

## References

### Research papers

- A.M. Betancourt, V. Berman, W. Herber, E. Katz, (1992) Analysis of tyrosinase synthesis in *Streptomyces antibioticus*. *J. Gen. Microbiol.* 138 : 787–794.
- Emilia Selinheimo *et al.*, (2007). Comparison of the characteristics of fungal and plant tyrosinases. *Journal of Biotechnology.* 130: 471–480.
- H. Claus (2003) Laccases and their occurrence in prokaryotes, *Arch. Microbiol.* 179: 145–150.
- H. Claus, Z. Filip (1988) Behaviour of phenoloxidases in the presence of clays and other soil-related adsorbents. *Appl. Microbiol. Biotechnol.* 28: 506–511.
- H. Claus, Z. Filip (1990) Enzymatic oxidation of some substituted phenols and aromatic amines, and the Behaviour of some phenoloxidases in the presence of soil related adsorbents. *Water Sci. Technol.* 22: 69–77.
- Herald claus and Heinz Decker (2006) Bacterial tyrosinase. *Systematic and Applied Microbiology.* 29: 3–14.
- L. Bubacco *et al.*, (1999) 1H NMR spectroscopy of the binuclear Cu(II) active site of *Streptomyces antibioticus* tyrosinase. *FEBS Lett.* 442: 215–220.
- L. Bubacco *et al.*, (2003) Spectroscopic characterization of the electronic changes in the active site of *Streptomyces antibioticus* tyrosinase upon binding of transition state analogue inhibitors. *J. Biol. Chem.* 278: 7381–7389.
- L. Cerenius, K. Soderhall (2004) The prophenoloxidase-activating system in invertebrates. *Immunol. Rev.* 198: 116–126.
- L.Y. Chen *et al.*, (1993) Mutational study of *Streptomyces* tyrosinase transactivator MelC1: MelC1 is likely a chaperone for apotyrosinase. *J. Biol. Chem.* 268 18,710–18,716.
- L.Y. Chen, W.M. Leu, K.T. Wang, Y.H. Lee (1992) Copper transfer and activation of the *Streptomyces* apotyrosinase are mediated through a complex formation between apotyrosinase and its transactivator MelC1, *J. Biol. Chem.* 267: 20,100–20,107.
- M.A. Marti-Renom, A. Stuart, A. Fiser, R. Sánchez, F. A. Melo, A. Sali (2000) Comparative protein structure modeling of genes and genomes. *Annu. Rev. Biophys. Biomol. Struct.* 29: 291–325.
- M.E. Arias, M. Arenas, M. Rodríguez, J. Soliveri, A.S. Ball, M. Herna´

nde, M. Kraft (2003) Pulp bleaching and mediated oxidation of a nonphenolic substrate by laccase from *Streptomyces cyaneus* CECT 3335. *Appl. Environ. Microbiol.* 69: 1953–1958.

Ning Wang and Daniel N. Hebert (2006) Tyrosinase maturation through the mammalian secretory pathway: bringing color to life. *Pigment Cell Res.* 19: 3–18.

Ram K. Tripathi, Vincent J. Hearing, Kazunori Urabe, Pilar Aroca, and Richard A. Spritz (1992) Mutational Mapping of the Catalytic Activities of Human Tyrosinase. *THE Journal of Biological Chemistry.* 267: 23707-23712.

Robert J. Deeth and Christian Diedrich (2010) Structural and mechanistic insights into the oxy form of the tyrosinase from molecular dynamics simulations. *J Biol Inorg Chem* 15: 117-129.

S. Castro-Sowinski, K. Martinez-Drets, Y. Okon (2002) Laccase activity in melanin-producing strains of *Sinorhizobium meliloti*. *FEMS Microbiol. Lett.* 209: 119–125.

S. Halaoui, M. Asther, J.-C. Sigoillot, M. Hamdi and A. Lomascolo (2006) Fungal tyrosinases: new prospects in molecular characteristics, bioengineering and biotechnological applications. *Journal of Applied Microbiology.* 5072: 219-232 .

Thorsten Schweikardt, Concepcion Olivares, Francisco Solano, Elmar Jaenicke, Jose Carlos Garcia-Borron and Heinz Decke (2007) A three dimensional model for mammalian tyrosinase active site accounting for loss of functions mutations. *pigment cell Res.* 20: 394-401.

V. Bernan, D. Filipula, W. Herber, M. Bibb, E. Katz (1985) The nucleotide sequence of the tyrosinase gene from *Streptomyces antibioticus* and characterization of the gene product. *Gene* 37: 101–110.

Vincent J. Hearing and Thomas M. Ekel (1976) A comparison of tyrosine hydroxylation and melanin formation. *Biochem. J.* 157: 549-557

Wuxian Shi et al., (2011) Metalloproteomics: Forward and Reverse approaches in metalloprotein structural and functional characterization. *Current Opinion in Chemical Biology.* 15: 144–148.

#### Software References

Andrea Passerini et al., (2012) Predicting Metal-Binding Sites from Protein Sequence. *TCBB.* 9: 203-213

A. Pedretti, L. villa, G. vistoli (2002) VEGA: a versatile program to convert, handle and visualize molecular structure on windows-based pcs. *J. Mol. Graph.* 21: 47-49.

A. Passerini, M. Punta, A. Ceroni, B. Rost, and P. Frasconi (2006) Identifying Cysteines and Histidines in Transition-Metal-Binding Sites Using Support Vector Machines and Neural Networks. *Proteins: Structure, Function, and Bioinformatics.* 65(2): 305-316.

Babor M, Gerzon S, Rahev B, Sobolev V, Edelman M. (2008) Prediction of transition metal-binding sites from apo protein structures. *Proteins.* 70: 208-217.

Humphrey, W., Dalke, A. and Schulten, K. (1996) VMD - Visual Molecular Dynamics. *J. Molec. Graphics.* 14: 33-38.

James C. Phillips, Rosemary Braun, Wei Wang, James Gumbart, Emad Tajkhorshid, Elizabeth Villa, Christophe Chipot, Robert D. Skeel, Laxmikant Kale, and Klaus Schulten (2005) Scalable molecular dynamics with NAMD. *Journal of Computational Chemistry.* 26:1781-1802.

Roger A. Sayle and E. James Milner-White (1995). *RasMol: Biomolecular graphics for all.* *Trends in Biochemical Sciences.* 20: 374-376.

Sali, A., Potterton, L., Yuan, F., van Vlijmen, H., & Karplus, M. (1995) Evaluation of comparative protein modelling by MODELLER. *Proteins.* 23: 318-326.

M. Lippi, A. Passerini, M. Punta, B. Rost, P. Frasconi. (2008) MetalDetector: a web server for predicting metal binding sites and disulfide bridges in proteins from sequence. *Bioinformatics.* 24(18): 2094-2095.

Torsten Schwede, Jurgen Kopp, Nicolas Guex and Manuel C. Peitsch (2003) SWISS-MODEL: an automated protein homology-modeling server. *Nucl. Acids Res.* 31(13): 3381-3385.

#### Books

Dominik Marx and Jurg Hutter (2009) *Ab initio Molecular Dynamics: Basic theory and advanced methods*, Cambridge University Press.

Ying Xu, Dong Xu and Jie Liang (2007) *Computational methods for protein structure prediction and Modeling (Volume 1) : Basic Characterization*, Springer.

Ivano Bertini, Astrid Sigel and Helmut Sigel (2001) *Handbook of Metalloproteins*, Marcel Dekker Inc.

Zhijun Wu (2007) *Lecture notes on computational structural biology*, World Scientific press.

Mohammed Zaki and Christopher Bystroff (2008) *Protein Structure prediction*, Humana Press.